Supporting Information

Influence of the Supported Ionic-Liquid Layer Thickness on *Z*-Selectivity in 1-Alkyne Hydrosilylation under Continuous Flow

André Böth[a], Florian Kaltwasser[a], Christian Priedigkeit[a], Boshra Atwi[b], Wolfgang Frey[c], Michael R. Buchmeiser[b]*, Ulrich Tallarek[a]*

[a] Department of Chemistry, Philipps-Universität Marburg, Hans-Meerwein-Strasse 4, 35032 Marburg, Germany

[b] Institute of Polymer Chemistry, Universität Stuttgart, Pfaffenwaldring 55, 70569 Stuttgart, Germany

[c] Institute of Organic Chemistry, Universität Stuttgart, Pfaffenwaldring 55, 70569 Stuttgart, Germany

---

* Corresponding authors.

Phone: +49 6421 28 25727; fax: +49 6421 28 27065.

E-mail address: tallarek@staff.uni-marburg.de (U. Tallarek).

URL: https://www.uni-marburg.de/fb15/ag-tallarek

Phone: +49 711 685 64074; fax: +49 711 685 64050.

E-mail address: michael.buchmeiser@ipoc.uni-stuttgart.de (M. R. Buchmeiser).

URL: https://www.ipoc.uni-stuttgart.de/msf/

Determination of the amount of solid silica in the microreactor

To ensure the accurate application of the IL and the adjustment of the SILP thickness (d_{SILP}), it is essential to determine the exact amount of solid silica present inside the microreactor. The volume of solid, i.e., impenetrable SiO_2 (V_{silica}) can be calculated by using the volume of the empty column (V_{column}) and the total porosity of the silica monolith (ε_{total})

$$V_{silica} = V_{column}(1 - \varepsilon_{total}) \tag{S1}$$

where V_{column} is calculated from the length (L_c) and radius (r_c) of the cylindrical column

$$V_{column} = \pi r_c^2 L_c \tag{S2}$$

The monolithic microreactor column has the dimensions of 4.6 mm i.d. × 100 mm length, which gives V_{column} = 1.662 mL. The total porosity is calculated according to

$$\varepsilon_{total} = \frac{t_{void} Q}{V_{column}} \tag{S3}$$

where t_{void} is the elution time of a passive tracer that does not interact with the surface and has access to the entire (macro–mesoporous) void volume V_{void} of the monolith (i.e., it functions as a dead-time marker) and Q is the volumetric flow rate. V_{void} is calculated from

$$V_{void} = t_{void} Q \tag{S4}$$

After combining Eqs. (S1), (S3), and (S4) the volume of the solid silica can be determined by

$$V_{silica} = V_{column} - V_{void} \tag{S5}$$

Therefore, a suitable dead-time marker has to be identified first, for which we tried several solutes. Because the surface of the monolithic microreactor consists of bare silica we used pure acetonitrile (ACN) as the mobile phase and a constant volumetric flow rate of Q = 0.75 mL/min. Figure S1 is a zoom into the elution curves obtained for the five different solutes we investigated as possible dead-time markers.

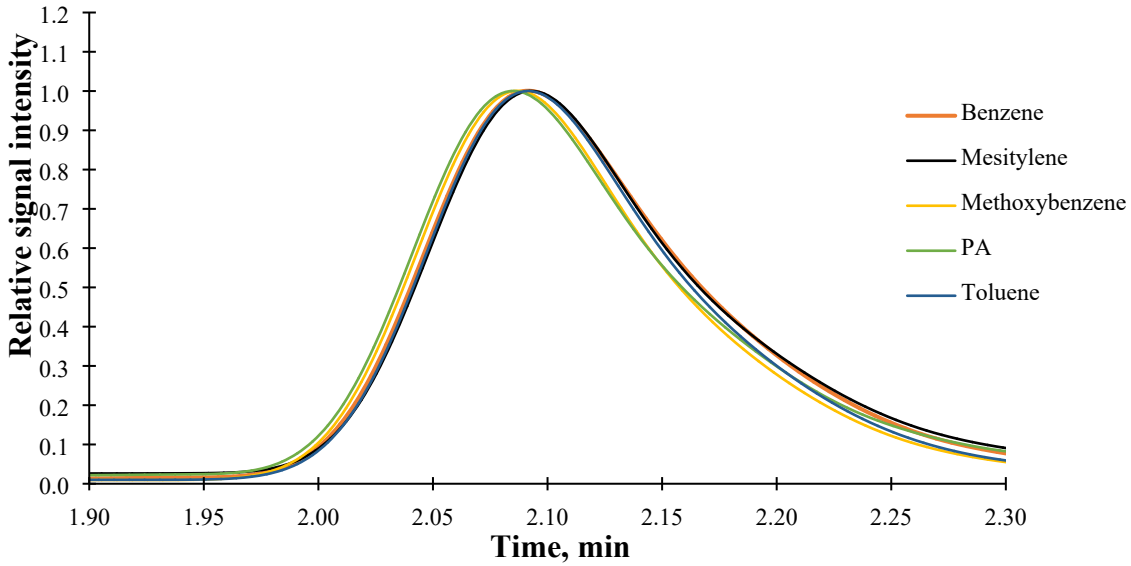

Figure S1. Elution curves of different solutes, normalized to their peak maximum for comparison, tested as potential dead-time markers (UV/Vis detection at λ = 260 nm). Standards were prepared in ACN and injected into ACN as mobile phase at Q = 0.75 mL/min.

No significant differences in dead times between the five markers were observed. For practical reasons, we chose phenylacetylene (PA) as dead-time marker. To determine the dead time of PA in the analytical system external to the microreactor (from the point of injection to detection), the monolithic microreactor was removed from the system and replaced by a zero-dead-volume union. The dead time inside the microreactor can then be calculated as

$$t_{void} = t_{reactor} - t_{external} \tag{S6}$$

By plotting the dead time of PA against the inverse volumetric flow rate of the solution (Figure S2) the slope of the regression curve can be used to determine the void volume V_{void} of the reactor in view of Eq. (S4). Relevant data from this experiment are summarized in Table S1.

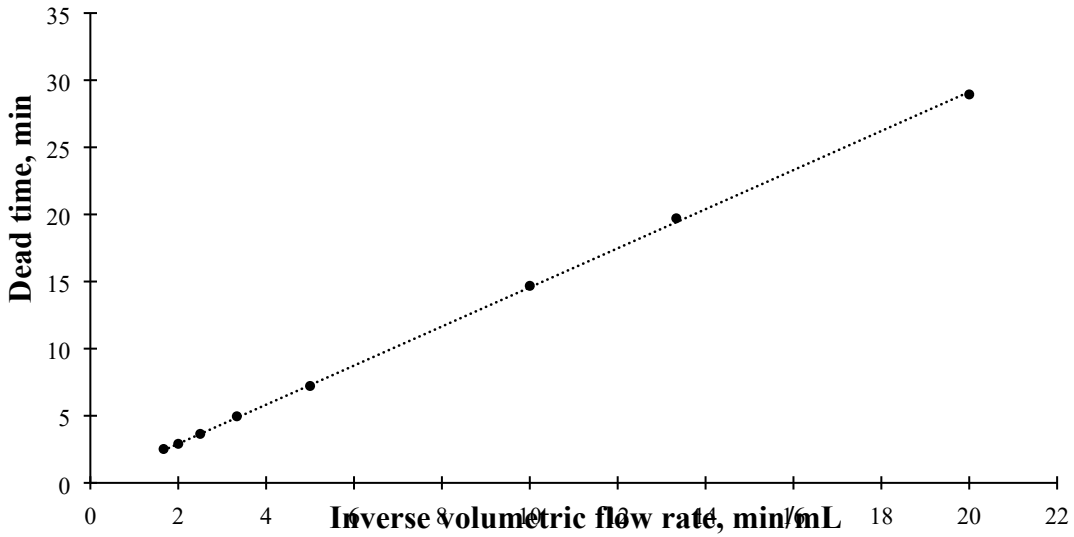

Figure S2. Determination of reactor void volume V_{void} from a plot of dead time (or void time, t_{void}) against the inverse volumetric flow rate ($1/Q$), cf. Eq. (S4).

Table S1. Parameters involved in the determination of the reactor void volume (V_{void}).

$1/Q$, min/mL	Q, mL/min	$t_{reactor}$, min	$t_{external}$, min	t_{void}, min
1.67	0.600	2.60	0.078	2.52
2.00	0.500	3.00	0.093	2.91
2.50	0.400	3.77	0.115	3.66
3.33	0.300	5.11	0.152	4.96
5.00	0.200	7.45	0.226	7.22
10.00	0.100	15.10	0.449	14.65
13.33	0.075	20.30	0.602	19.70
20.00	0.050	29.90	0.917	28.98

With V_{void} = 1.459 mL, the total porosity of the monolith can be calculated from

$$\varepsilon_{total} = \frac{V_{void}}{V_{column}} = \frac{1.459\ mL}{1.662\ mL} = 0.878$$

(S7)

Thus, the total void volume of the macro–mesoporous silica monolith as seen by PA is ~88%, in excellent agreement with previously published data for similar materials.[S1] Further, assuming a density of 2.2 g/cm^3 for the solid silica of the monolith, which is typical for this type of material,[S2] the mass of silica in the monolithic column, m_{silica}, is given by

$$m_{silica} = (V_{column} - V_{void}) \cdot \rho_{silica} \qquad \text{(S8)}$$

$$0.447\ g = \left(1.662\ cm^3 - 1.459\ cm^3\right) \cdot 2.2\ g\ cm^{-3}$$

Summarizing, the mass of solid, impermeable silica inside the monolithic microreactor is 0.447 g. With the known m_{silica} different SILP thicknesses can be adjusted according to

$$d_{SILP} = \frac{V_{IL}}{m_{silica} A_{meso}} \qquad \text{(S9)}$$

where A_{meso} = 110 m^2/g is the specific mesopore surface area of the monolith. In practice, a SILP thickness is specified and the corresponding V_{IL} calculated via Eq. (S9). The four SILP thicknesses and associated values of V_{IL} and $m_{\mathbf{Rh\text{-}1}}$ (mass of **Rh-1** dissolved in the SILPs) are summarized in Table S2.

Table S2. Volumes of the IL and amounts of catalysts used for the different SILP layers.

d_{SILP}, nm	V_{IL}, mL	$m_{\mathbf{Rh\text{-}1}}$, mg
1	0.0493	1.33
3	0.1480	4.00
5	0.2460	6.66
15	0.7400	20.00

Calibration curves for the $\beta(Z)$-isomer and the $\beta(E)$-isomer

These procedures are similar to previous studies.[S3] Calibration curves for the two compounds of interest in this work, the $\beta(Z)$-isomer and the $\beta(E)$-isomer (Figures S3 and S4), were required for quantification of the respective compounds based on their recorded chromatographic peaks. The

calibration solutions were prepared with the pure compounds as received through separation on a semi-preparative column (see further below). To minimize the amount of substance required for calibration, the procedure was conducted using an autosampler. Subsequently, the sample volume injected with the autosampler was varied, covering the relevant range of sample amounts received during microreactor operation. Conditions adapted for the generation of the calibration curves were identical to those encountered during the reactor screening. Duplicate measurements were used for each reported point. Individual data points for the calibration curves were obtained from the area of a chromatographic peak (recorded at a wavelength of 260 nm) as well as the injection volume of the autosampler. All compounds exhibited linear behavior (signal area vs. the amount of injected substance) over the calibrated range.

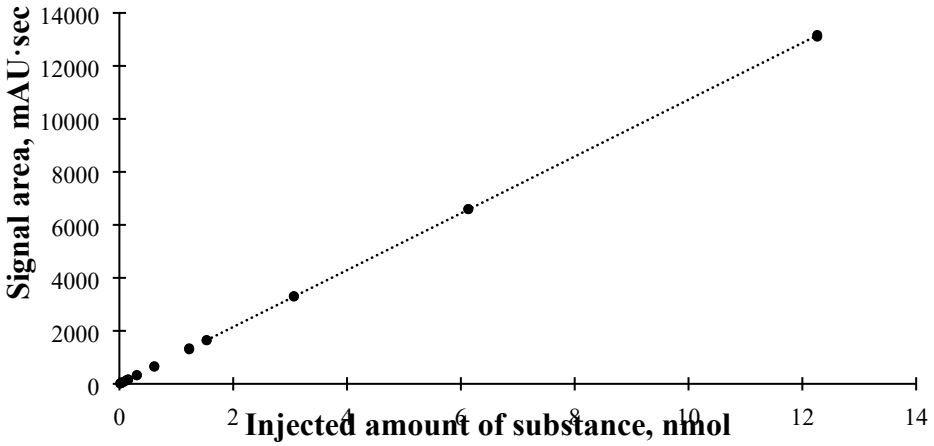

Figure S3. Calibration curve for the β(*Z*)-isomer (compound **4** of Scheme 2 in the main text) at a detection wavelength of 260 nm. Mobile phase: 75/25 (v/v) methanol/water.

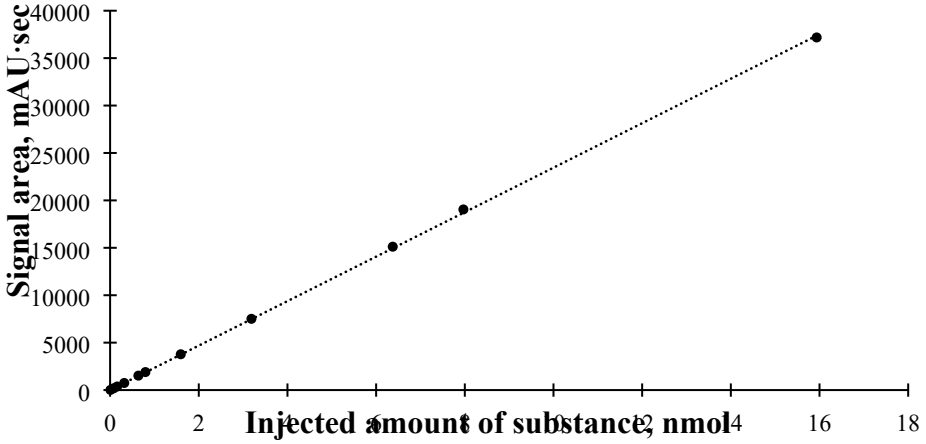

Figure S4. Calibration curve for the β(*E*)-isomer (compound **5** of Scheme 2 in the main text) at a detection wavelength of 260 nm. Mobile phase: 75/25 (v/v) methanol/water.

A comparison of UV/Vis spectra of the isomers encountered in the reaction monitoring is shown in Figure S5, revealing λ = 260 nm as a suitable detection wavelength.

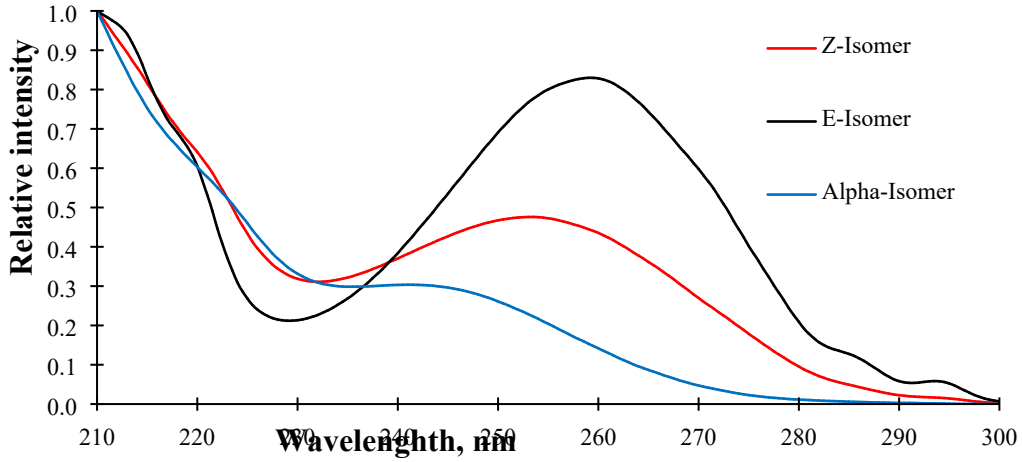

Figure S5. UV/Vis spectra for compounds **3**–**5** of Scheme 2 in the main text. For comparison, all spectra were normalized to intensity at λ = 210 nm.

Synthesis and semi-preparative separation/isolation of the $\beta(Z)$- and $\beta(E)$-isomers

$\beta(Z)$- and $\beta(E)$-isomers were synthesized according to an established protocol.[S4] The reaction was stirred overnight, the resulting solution diluted with methanol/water (v/v) 80/20 by a factor of two and then adjusted to pH 3.8 with formic acid. Semi-preparative isolation was achieved using a XSelect CSH Phenyl-Hexyl OBD Prep Column (10 mm i.d. × 250 mm length, 5 µm particle size, 13 nm mesopore size) equipped with an additional Guard Column XSelect CSH Phenyl-Hexyl Prep Guard Cartridge (10 mm i.d. × 10 mm length) from Waters Inc. (Milford, MA). The homogenous, clear, pale yellow, diluted reaction solution was directly injected through a 100 µL sample loop. Baseline separation of the isomers was achieved under isocratic conditions using a 76/24 (v/v) methanol/water mobile phase at pH 3.8. The volumetric flow rate was set to Q = 3.25 mL/min. A representative chromatogram is seen in Figure S6. The separation was repeated several times and the isomers were collected using a fraction collector.

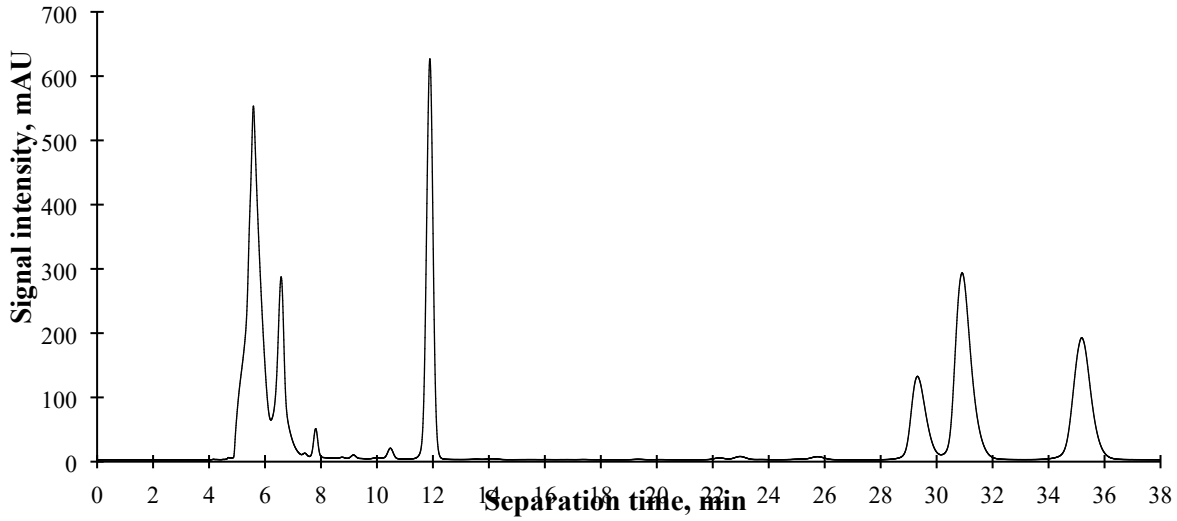

Figure S6. Representative chromatogram obtained with a semi-preparative-scale column under the conditions described in the text (detection at 260 nm). The three isomers elute in the following order: α-isomer (29 min), $\beta(Z)$-isomer (31 min), and $\beta(E)$-isomer (35 min).

β(*Z*)-1-Phenyl-2-dimethylphenylsilylethene (**4**): Purification by column liquid chromatography (XSelect CSH Phenyl-Hexyl OBD Prep Column, 10 mm i.d. × 250 mm length, 5 µm particle size, 13 nm mesopore size) yielded **4** as a yellow oil (retention time: 31 min, cf. Figure S6). NMR spectroscopic data were in accordance with those reported in the literature.[S4] **^{1}H NMR** (300 MHz, chloroform-*d*): δ = 7.60–7.50 (m, 4H), 7.40–7.30 (m, 6H), 6.98 (d, *J* = 15.1 Hz, 1H), 6.62 (d, *J* = 15.1 Hz, 1H), 0.47 (s, 6H).

β(*E*)-1-Phenyl-2-dimethylphenylsilylethene (**5**): Purification by column liquid chromatography (XSelect CSH Phenyl-Hexyl OBD Prep Column, 10 mm i.d. × 250 mm length, 5 µm particle size, 13 nm mesopore size) yielded **5** as a yellow oil (retention time: 35 min, cf. Figure S6). NMR spectroscopic data were in accordance with those reported in the literature.[S4] **^{1}H NMR** (300 MHz, chloroform-*d*): δ (ppm) = 7.66–7.57 (m, 2H), 7.50–7.45 (m, 2H), 7.45–7.30 (m, 6H), 6.98 (d, *J* = 19.2 Hz, 1H), 6.62 (d, *J* = 19.1 Hz, 1H), 0.47 (s, 6H). **^{13}C NMR** (101 MHz, $CDCl_3$): δ (ppm) = 149.17, 140.73, 140.69, 134.81, 131.28, 129.94, 129.36, 128.93, 128.57, 2.15.

[(1,3-Dimethyl-1*H*-imidazol-2-ylidene)(1,5-cyclooctadiene)rhodium(I) tetrafluoroborate] (Rh-2): $AgBF_4$ (14.2 mg, 0.073 mmol, 1 eq) in 2 mL pivalonitrile was added dropwise to a solution of [(1,3-dimethyl-1*H*-imidazol-2-ylidene)(1,5-cyclooctadiene)rhodium(I) chloride[S5] (25 mg, 0.073 mmol, 1 eq) in 2 mL pivalonitrile at -40 °C and the mixture was stirred at room temperature for 40 min. The solid precipitate was filtered off through a short plug of celite and the solvent was evaporated to dryness. The residue was washed with *n*-pentane (2 × 5 mL) and dried to yield the target product as a yellow solid. Yield: 78% (27 mg, 0.057 mmol). **^{1}H NMR** (400 MHz, CD_2Cl_2): δ (ppm) = 6.98 (d, *J* = 21.4 Hz, 2H), 4.79 (s, 2H), 4.02 (s, 6H), 3.83 (s, 2H) 2.46 (s, 4H), 2.09 (d, *J* = 9.2 Hz, 4H), 1.34 (s, 12H). **^{19}F NMR** (376 MHz, CD_2Cl_2): δ (ppm) = -153.26. **^{13}C NMR** (176 MHz, CD_2Cl_2): δ (ppm) = 178.6, 166.7, 145.4, 133.2, 132.0, 128.3, 121.6, 120.2, 59.4, 50.7, 25.6, 21.0, 20.0, 6.6. **HRMS** calculated for $[M]^+$: $C_{18}H_{29}N_3Rh$: 390.1411, found: 390.1388. **Anal. Calc.** for $C_{18}H_{29}BF_4N_3Rh$: C, 45.31; H, 6.13; N, 8.81. Found: C, 45.33; H, 6.45; N, 8.90.

Continuous-flow hydrosilylation with Rh-3 and a SILP thickness of 1 nm: The column was impregnated with a solution of 0.8 mg **Rh-3** in 50 µL [BMIM][BF_4] and 1.45 mL of CH_2Cl_2. The solvent was removed overnight *in vacuo*, followed by flushing the column with 15 mL MTBE.

Table S3. Weights and moles of the β(*Z*)-isomer involved in the comparison to the produced β(*Z*)- and β(*E*)-isomers reported in Figures 5 and 6 of the main text.[a]

time [min]	15 nm		5 nm		3 nm		1 nm	
	m [ng]	*n* [µmol]	*m* [ng]	*n* [µmol]	*m* [ng]	*n* [µmol]	*m* [ng]	*n* [µmol]
20.2	0.093	0.391	0.033	0.138	0.042	0.174	0.026	0.109
73.2	0.060	0.252	0.020	0.086	0.030	0.126	0.017	0.071
126.2	0.037	0.154	0.016	0.066	0.023	0.097	0.017	0.071
179.2	0.029	0.123	0.015	0.062	0.021	0.089	0.024	0.101
232.2	0.025	0.104	0.014	0.058	0.019	0.080	0.029	0.122
285.2	0.021	0.086	0.014	0.057	0.018	0.077	0.031	0.130
338.2	0.022	0.092	0.015	0.063	0.017	0.070	0.032	0.134
391.2	0.019	0.078	0.014	0.058	0.016	0.068	0.031	0.130
444.2	0.018	0.074	0.015	0.062	0.015	0.064	0.031	0.130
497.2	0.017	0.070	0.016	0.065	0.014	0.060	0.03	0.126
550.2	0.016	0.066	0.015	0.063	0.014	0.059	0.031	0.130
603.2	0.015	0.063	0.013	0.056	0.014	0.057	0.031	0.130

[a] The values reported for weights and moles of the β(*Z*)- and β(*E*)-isomer are small (in the ng- and µmol-range, respectively), because they reflect chromatographically determined yields. Only 2.57 µL of the reaction solution from the microreactor (1st dimension) were transferred via the 2-position/6-port (injection) valve into the second dimension of the experimental setup shown in Figure 3 for subsequent chromatographic separation and detection.

Table S4. Weights and moles of the β(*E*)-isomer involved in the comparison to the produced β(*Z*)- and β(*E*)-isomers reported in Figures 5 and 6 of the main text.[a]

time [min]	15 nm		5 nm		3 nm		1 nm	
	m [ng]	*n* [µmol]	*m* [ng]	*n* [µmol]	*m* [ng]	*n* [µmol]	*m* [ng]	*n* [µmol]
20.2	1.553	6.513	0.189	0.791	0.141	0.590	0.101	0.424
73.2	1.342	5.628	0.118	0.496	0.096	0.401	0.059	0.247
126.2	0.998	4.188	0.085	0.356	0.066	0.275	0.052	0.218
179.2	0.784	3.290	0.071	0.300	0.052	0.219	0.051	0.214
232.2	0.660	2.767	0.059	0.247	0.043	0.180	0.045	0.189
285.2	0.578	2.425	0.053	0.222	0.038	0.160	0.039	0.164
338.2	0.522	2.191	0.052	0.218	0.033	0.139	0.034	0.143
391.2	0.477	2.002	0.042	0.178	0.030	0.125	0.031	0.130
444.2	0.440	1.846	0.042	0.175	0.027	0.112	0.028	0.117
497.2	0.410	1.719	0.040	0.168	0.025	0.106	0.027	0.113
550.2	0.384	1.611	0.036	0.151	0.024	0.099	0.024	0.101
603.2	0.364	1.526	0.030	0.124	0.022	0.092	0.023	0.096

[a] The values reported for weights and moles of the β(*Z*)- and β(*E*)-isomer are small (in the ng- and µmol-range, respectively), because they reflect chromatographically determined yields. Only 2.57 µL of the reaction solution from the microreactor (1st dimension) were transferred via the 2-position/6-port (injection) valve into the second dimension of the experimental setup shown in Figure 3 for subsequent chromatographic separation and detection.

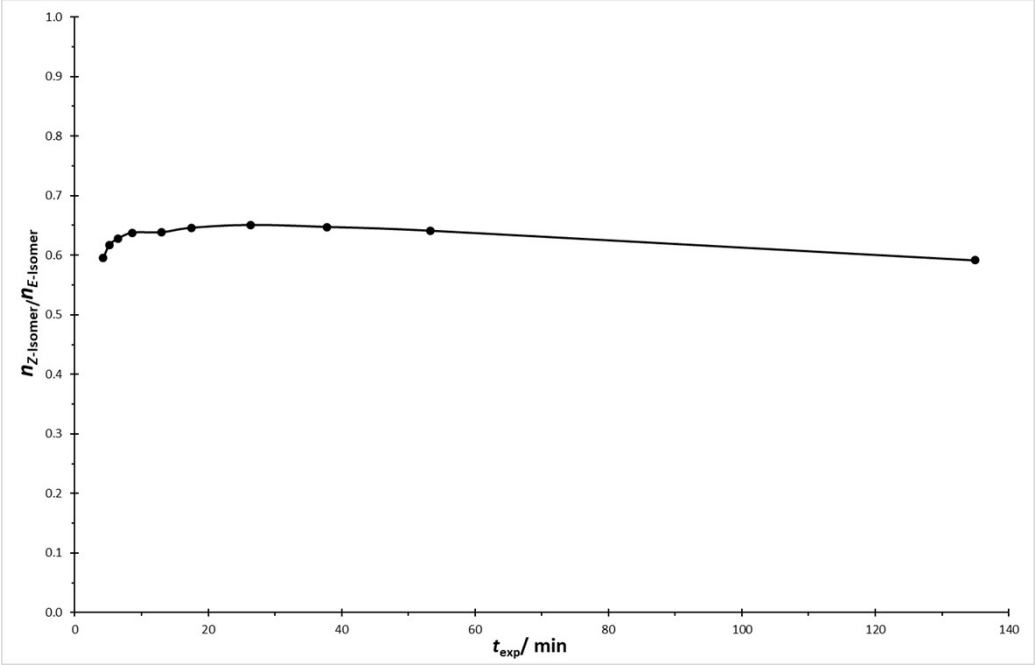

Figure S7. *Z*/*E*-selectivity in the hydrosilylation of PA with DMPS over the course of 140 minutes using **Rh-2** in combination with a 1 nm-thick SILP.

Table S5. Hydrosilylation with **Rh-3**. MTBE solution with 25 mM PA and 32.5 mM DMPS was injected onto the monolithic, **Rh-3**-containing column (1.4 mg **Rh-3**/50 µL IL) at 50 °C applying a flow rate of 0.066 mL/min. Samples were taken in 20 min intervals and characterized through GC-MS.

Time [min]	α / β(*Z*) / β(*E*)	β(*Z*) / β(*E*) ratio
40	59/0/41	0
60	28/4/68	0.059
80	33/3/64	0.047
100	28/3/69	0.043
120	28/3/69	0.043
140	29/4/67	0.060
160	28/3/69	0.043
180	28/3/69	0.043
200	26/4/70	0.057
220	27/3/70	0.043
240	28/4/68	0.059
260	29/5/66	0.076
280	31/4/65	0.062
300	31/5/64	0.077
320	32/3/65	0.046
340	31/5/64	0.077
360	32/5/63	0.079
380	33/5/62	0.081
400	33/5/62	0.081
420	34/5/62	0.081
440	34/5/62	0.081
460	35/6/59	0.102
480	35/6/59	0.102
500	35/6/59	0.102
520	34/7/59	0.119
540	35/6/59	0.102

NMR Spectra

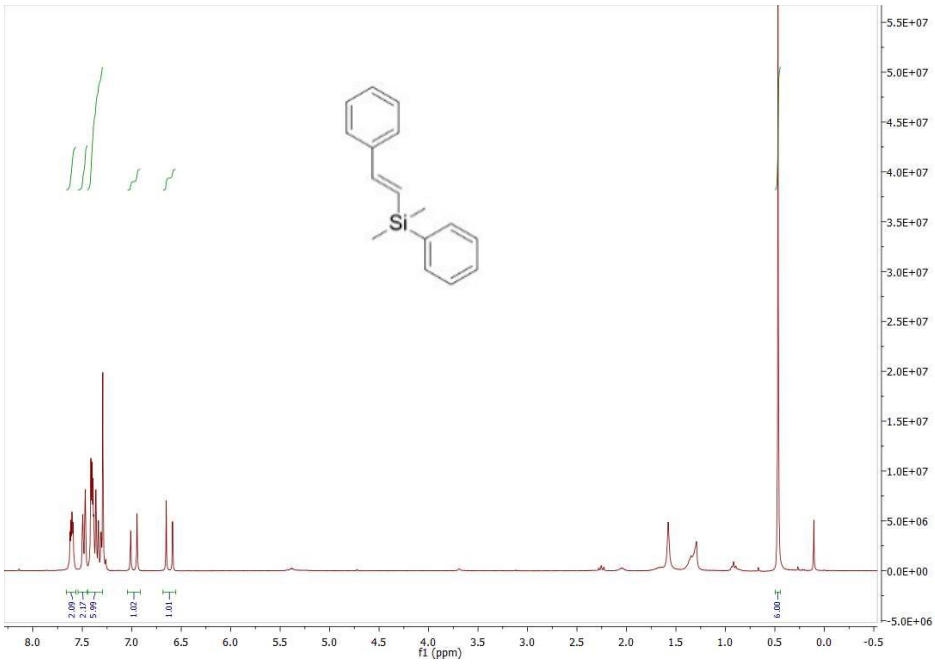

Figure S8. ^{1}H NMR spectrum (300 MHz, $CDCl_3$) of β(*E*)-1-phenyl-2-dimethylphenylsilylethene.

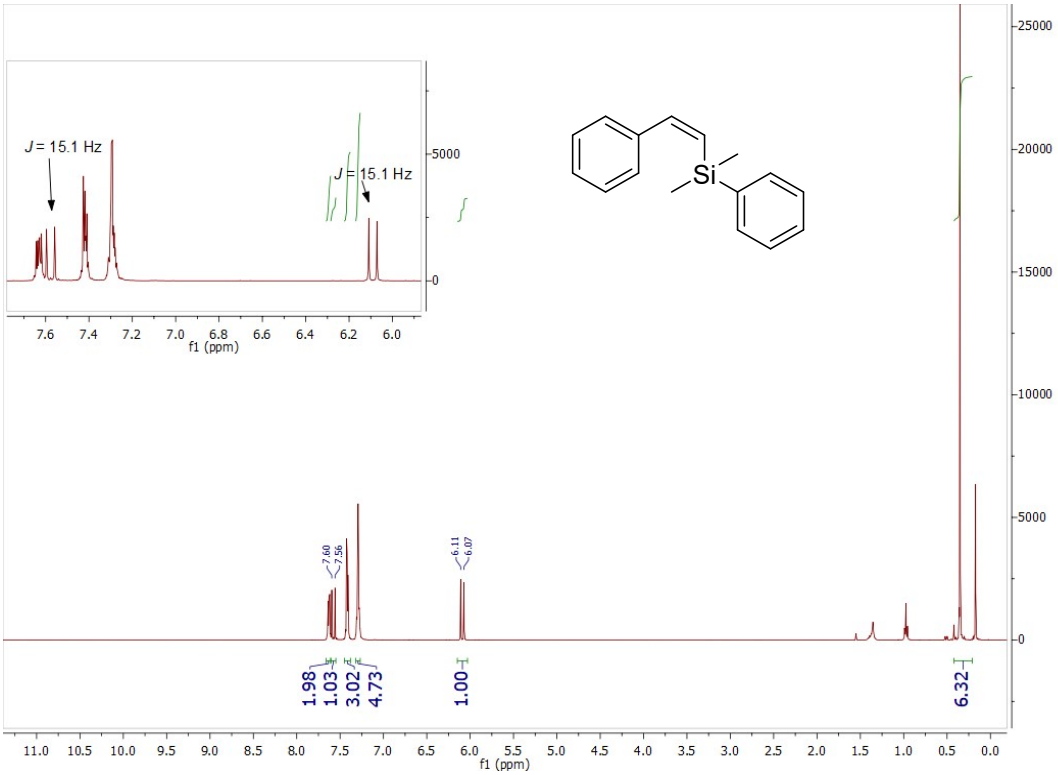

Figure S9. ^{1}H NMR spectrum (400 MHz, $CDCl_3$) of β(*Z*)-1-phenyl-2-dimethylphenylsilylethene.

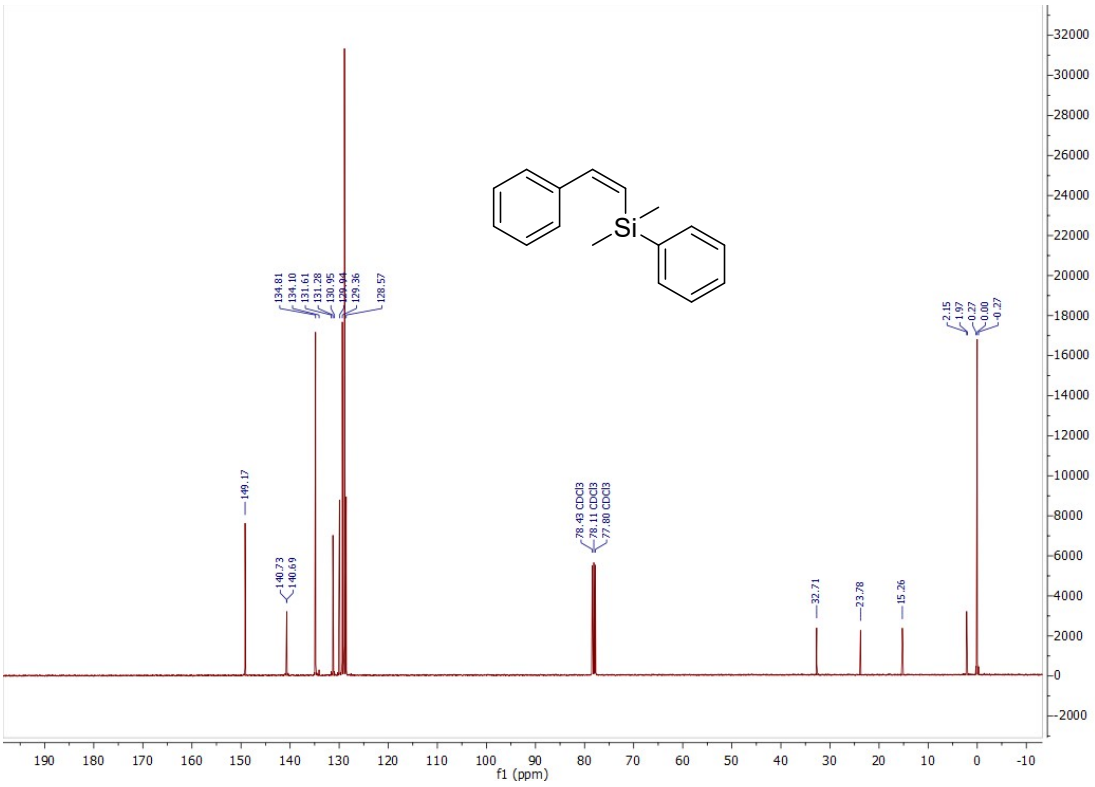

Figure S10. ^{13}C NMR spectrum (101 MHz, $CDCl_3$) of (*Z*)-1-phenyl-2-dimethylphenylsilylethene.

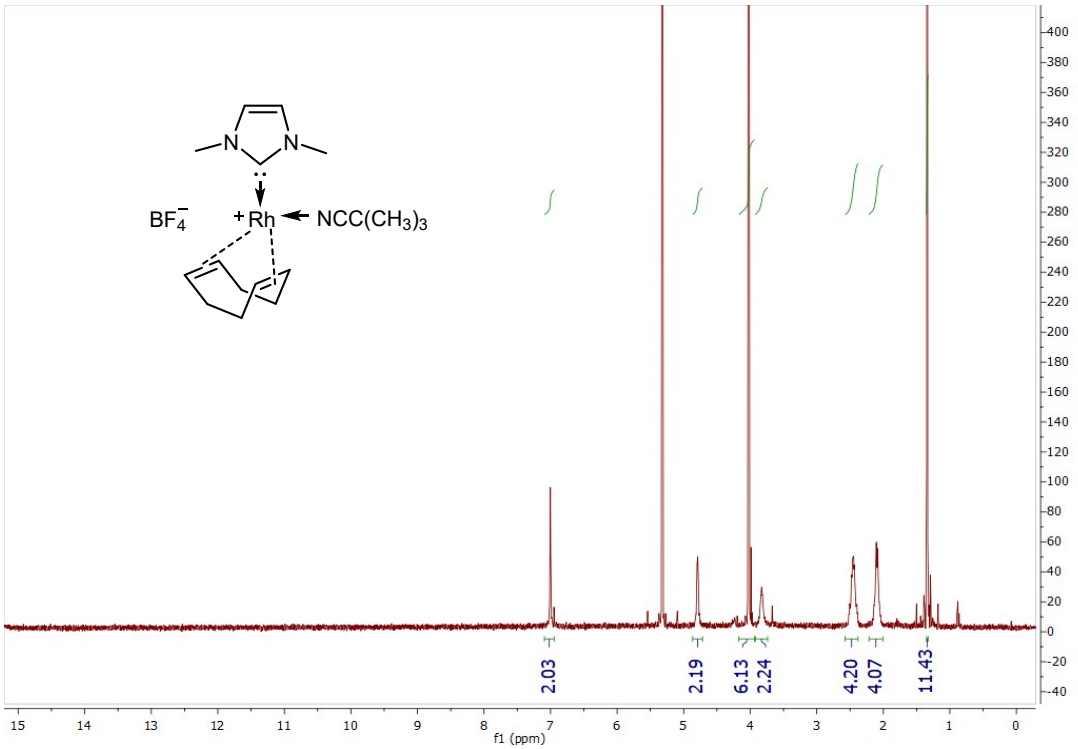

Figure S11. ^{1}H NMR spectrum (400 MHz, CD_2Cl_2) of **Rh-2**.

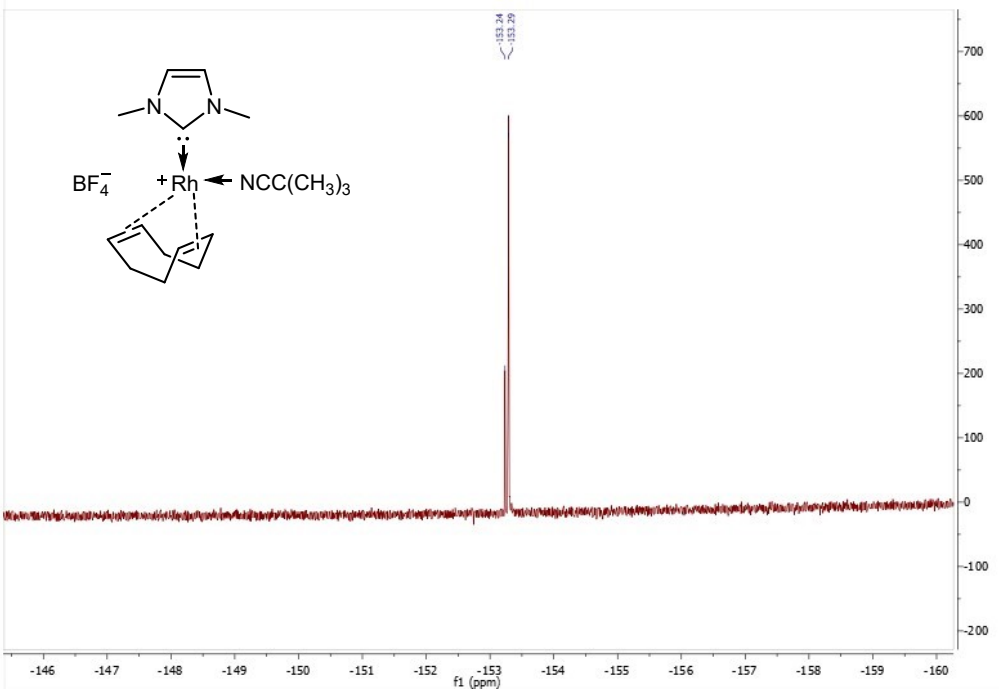

Figure S12. ^{19}F NMR spectrum (400 MHz, CD_2Cl_2) of **Rh-2**.

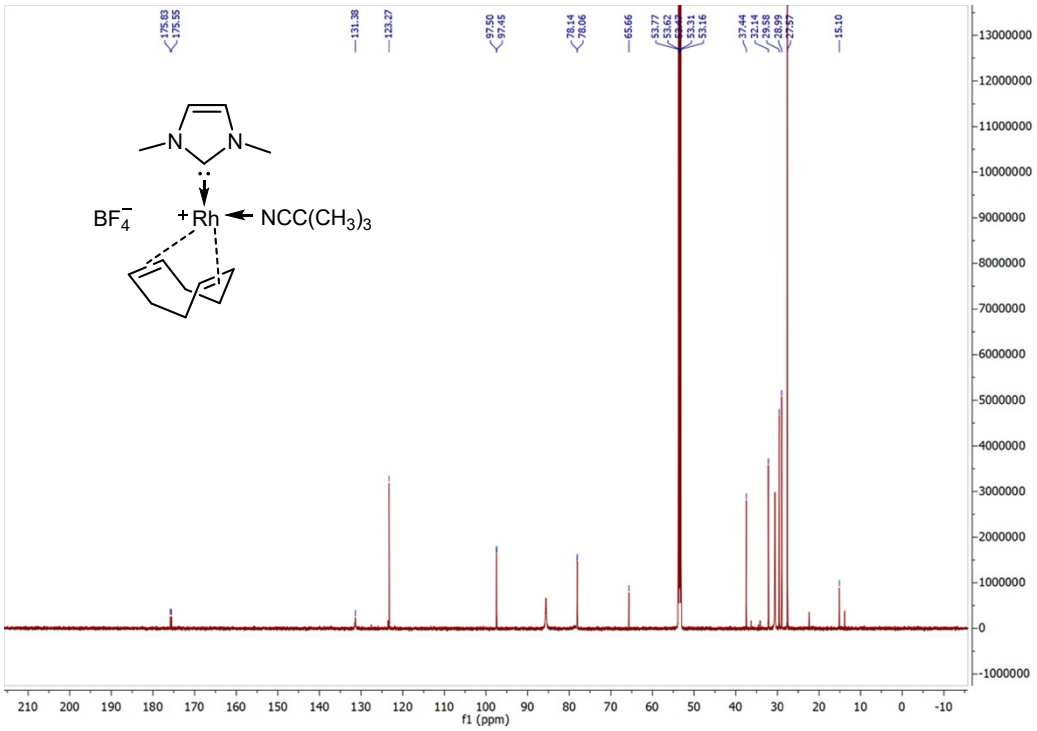

Figure S13. ^{13}C NMR spectrum (175 MHz, CD_2Cl_2) of **Rh-2**.

Attempted isomerization of (*Z*)-1-phenyl-2-dimethylphenylsilylethene by Rh-3: The (still active) **Rh-3**-containing monolithic column used for hydrosilylation was flushed with pure MTBE until no peaks from substrates and products occurred in the GC-MS chromatogram. To check the possibility of catalyst-induced product isomerization under continuous flow, a solution of isolated (*Z*)-1-phenyl-2-dimethylphenylsilylethene in MTBE was injected at a flow rate of 0.066 µL/min onto the microreactor placed in a thermostatted column compartment (50 °C). The eluent was analyzed via GC-MS. The obtained GC-MS data are represented in **Figure S14**. No isomerization was observed and the same product distribution obtained with the same retention time for the β(*Z*)-isomer (t_r = 9.65 min).

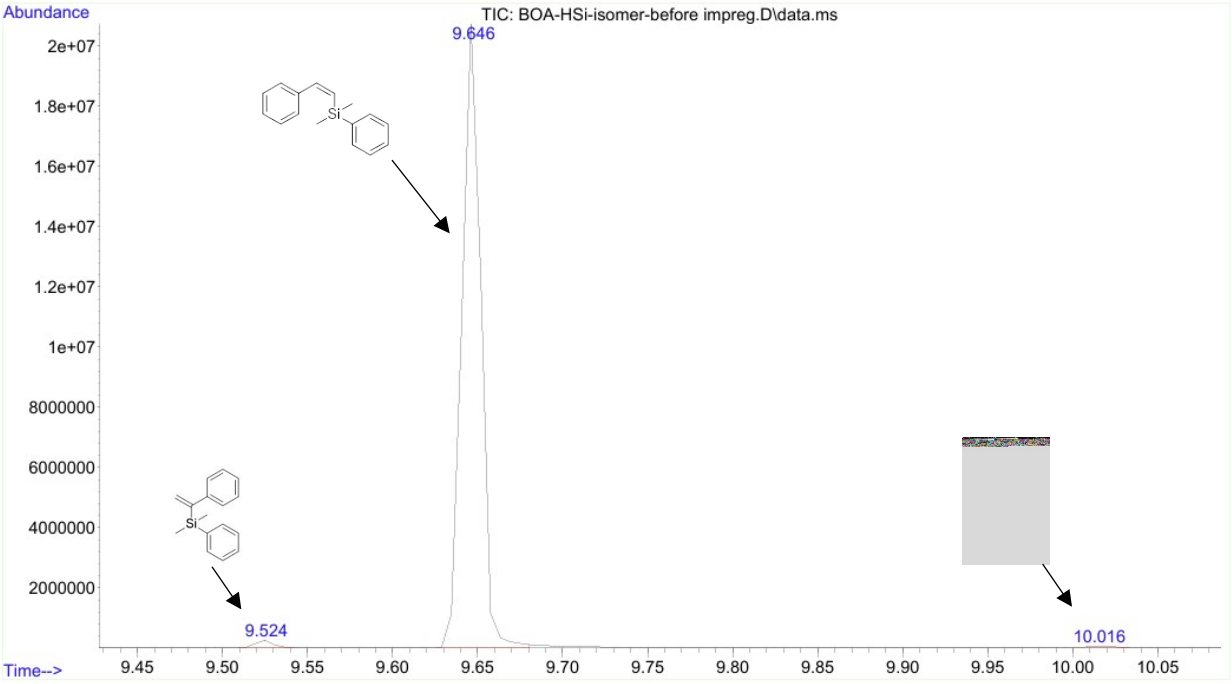

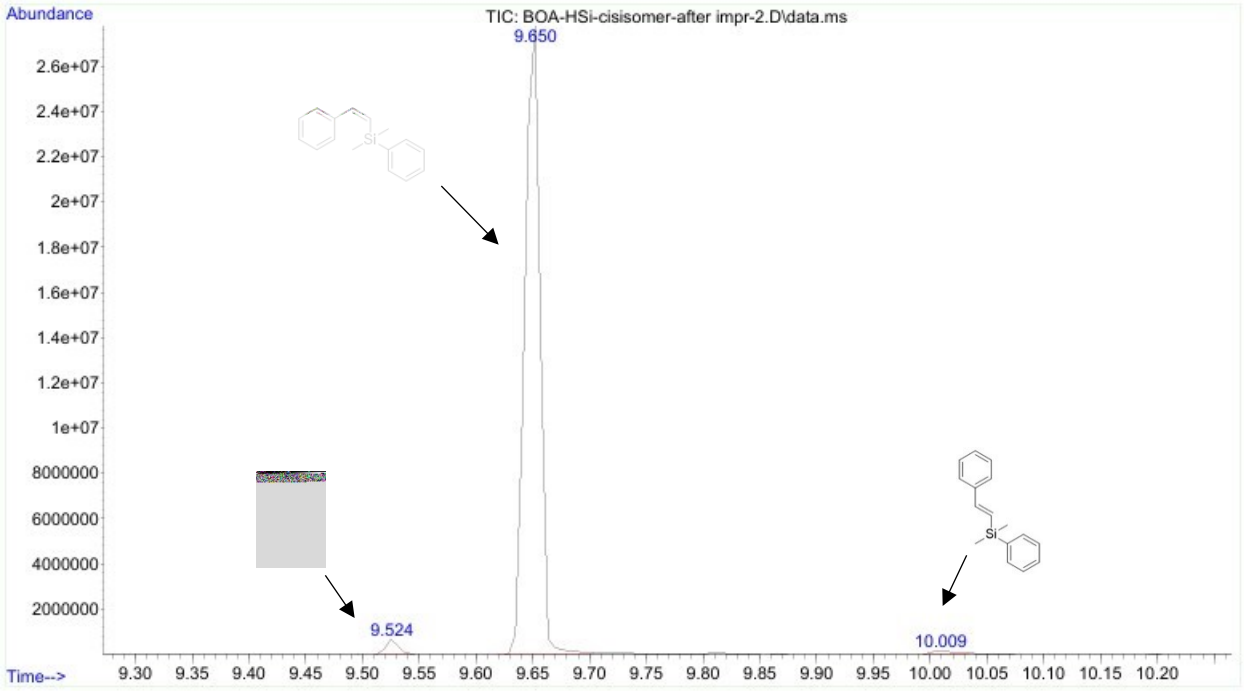

Figure S14. GC-MS chromatogram before (top) and after injection (bottom) of the β(*Z*)-isomer onto the monolithic column.

X-Ray Data

Table S6. Crystal data and structure refinement for **Rh-1**.

Empirical formula	C26 H31 B Cl2 F4 N3 Rh	
Formula weight	646.16 g/mol	
Temperature	100(2) K	
Wavelength	0.71073 Å	
Crystal system, space group	Triclinic, P-1	
Unit cell dimensions	a = 9.756(5) Å	alpha = 75.446(16)°
	b = 11.147(5) Å	beta = 83.737(16)°
	c = 13.527(7) Å	gamma = 73.626(17)°
Volume	1364.9(12) $Å^3$	
Z, Calculated density	2, 1.572 Mg/m^3	
Absorption coefficient	0.870 mm^{-1}	
F(000)	656	
Crystal size	0.140 x 0.090 x 0.040 mm	
Theta range for data collection	1.957 to 24.248°	
Limiting indices	-11<=h<=11, -12<=k<=12, -15<=l<=15	
Reflections collected / unique	15749 / 4373 [R(int) = 0.1795]	
Completeness to Θ= 24.248°	99.1 %	
Absorption correction	Semi-empirical from equivalents	
Max. and min. transmission	0.7096 and 0.5790	
Refinement method	Full-matrix least-squares on F^2	
Data / restraints / parameters	4373 / 48 / 338	
Goodness-of-fit on F^2	1.040	
Final R indices [I>2σ(I)]	R1 = 0.0835, wR2 = 0.1421	
R indices (all data)	R1 = 0.1744, wR2 = 0.1602	
Extinction coefficient	0.0153(12)	
Largest diff. peak and hole	1.518 and -1.000 $e.Å^{-3}$	

Table S7. Crystal data and structure refinement for **Rh-2**.

Empirical formula	C18 H29 B F4 N3 Rh	
Formula weight	477.16	
Temperature	100(2) K	
Wavelength	0.71073 Å	
Crystal system, space group	monoclinic, C2	
Unit cell dimensions	a = 20.6843(17) Å	alpha = 90°
	b = 8.2612(6) Å	beta = 117.168(7)°
	c = 15.1611(13) Å	gamma = 90°
Volume	2304.9(3) $Å^3$	
Z, Calculated density	4, 1.375 Mg/m^3	
Absorption coefficient	0.779 mm^{-1}	
F(000)	976	
Crystal size	0.397 x 0.139 x 0.127 mm	
Theta range for data collection	2.031 to 28.423°	
Limiting indices	-27<=h<=27, -11<=k<=10, -20<=l<=20	
Reflections collected / unique	20767 / 5735 [R(int) = 0.0262]	
Completeness to Θ= 25.242	100.0 %	
Absorption correction	Semi-empirical from equivalents	
Max. and min. transmission	0.7457 and 0.6662	
Refinement method	Full-matrix least-squares on F^2	
Data / restraints / parameters	5735 / 61 / 264	
Goodness-of-fit on F^2	1.056	
Final R indices [I>2σ(I)]	R1 = 0.0293, wR2 = 0.0669	
R indices (all data)	R1 = 0.0359, wR2 = 0.0702	
Absolute structure parameter	0.51(7)	
Extinction coefficient	n/a	
Largest diff. peak and hole	1.152 and -1.004 $e·Å^{-3}$	

****

Disordered solvent density (CH_2Cl_2) eliminated with squeeze (PLATON)!

****

References

[S1] K. Hormann, U. Tallarek, *J. Chromatogr. A* 2014, **1365**, 94-105.

[S2] a) A. Galarneau, Z. Abid, B. Said, Y. Didi, K. Szymanska, A. Jarzębski, F. Tancret, H. Hamaizi, A. Benguedda ch, F. Di Renzo, F. Fajula, *Inorganics* 2016, **4**, 9; b) H. U. K. Jatoi, M. Goepel, D. Poppitz, R. Kohns, D. Enke, M. Hartmann, R. Gläser, *Front. Chem Eng.* 2021, **3**, 789416.

[S3] a) C. P. Haas, T. Müllner, R. Kohns, D. Enke, U. Tallarek, *React. Chem. Eng.* 2017, **2**, 498-511; b) A. Böth, T. Roider, F. Ziegler, X. Xie, M. R. Buchmeiser, U. Tallarek, *ChemCatChem* 2023, **15**, e202201268.

[S4] P. R. K. Panyam, B. Atwi, F. Ziegler, W. Frey, M. Nowakowski, M. Bauer, M. R. Buchmeiser, *Chem. Eur. J.* 2021, **27**, 17220-17229.

[S5] I. M. Daubit, M. P. Sullivan, M. John, D. C. Goldstone, C. G. Hartinger, N. Metzler-Nolte, *Inorg. Chem.* 2020, **59**, 17191-17199.